Received: 26 September 2021 | Revised: 26 September 2021 | Accepted: 1 October 2021

DOI: 10.1002/psp4.12732

ARTICLE

Pharmacometric analysis of seasonal influenza epidemics and the effect of vaccination using sentinel surveillance data

Yuki Otani[1,2] | **Hidefumi Kasai**[1] | **Yusuke Tanigawara**[1]

[1]Laboratory of Pharmacometrics and Systems Pharmacology, Keio Frontier Research and Education Collaboration Square at Tonomachi, Kanagawa, Japan

[2]Keio University Graduate School of Medicine, Tokyo, Japan

Correspondence
Yusuke Tanigawara, Laboratory of Pharmacometrics and Systems Pharmacology, Keio Frontier Research and Education Collaboration Square (K-FRECS) at Tonomachi, Keio University, Research Gate Building TONOMACHI 2-A, 3-25-10 Tonomachi, Kawasaki-ku, Kawasaki, Kanagawa 210-0821, Japan.
Email: tanigawara@keio.jp

Funding information
No funding was received for this work.

Abstract

The identification of influenza epidemics and assessment of the efficacy of vaccination against this infection are major challenges for the implementation of effective public health strategies, such as vaccination programs. In this study, we developed a new pharmacometric model to evaluate the efficacy of vaccination based on infection surveillance data from the 2010/2011 to 2018/2019 influenza seasons in Japan. A novel susceptible-infected-removed plus vaccination model, based on an indirect response structure with the effect of vaccination, was applied to describe seasonal influenza epidemics using a preseasonal collection of data regarding serological H_1 antibody titer positivity and the fraction of virus strains. Using this model, we evaluated K_{in} (a parameter describing the transmission rate of symptomatic influenza infection) for different age groups. Furthermore, we defined a new parameter (prevention factor) showing the efficacy of vaccination against each viral strain and in different age groups. We found that the prevention factor of vaccination against influenza varied among age groups. Notably, children aged 5–14 years showed the highest K_{in} value during the 10 influenza seasons and the greatest preventive effect of vaccination (prevention factor = 70.8%). The propagation of influenza epidemics varies in different age groups. Children aged 5–14 years most likely play a leading role in the transmission of influenza. Prioritized vaccination in this age group may be the most effective strategy for reducing the prevalence of influenza in the community.

Study Highlights

WHAT IS THE CURRENT KNOWLEDGE ON THE TOPIC?

A traditional susceptible-infected-removed (SIR) model using sentinel surveillance data has been applied to the analysis of influenza epidemics and the effect of preventive measures, such as social distancing. However, quantitative analysis has not been performed.

WHAT QUESTION DID THIS STUDY ADDRESS?

Can we evaluate the efficacy of vaccination for seasonal influenza over different strains of virus using a quantitative modeling approach? Which age group is the most important in the preventive strategy for seasonal influenza?

WHAT DOES THIS STUDY ADD TO OUR KNOWLEDGE?

An incorporation of a pharmacometric modeling approach to the epidemiological data was done to address the dynamics of influenza infection and effect of vaccination. During the 2010–2019 seasons, children aged 5–14 years showed the highest transmission rate of influenza and preventive effect of vaccination.

HOW MIGHT THIS CHANGE DRUG DISCOVERY, DEVELOPMENT, AND/OR THERAPEUTICS?

By using the current SIR plus vaccination model, we quantitatively analyzed the transmission of influenza and the efficacy of treatment modalities (e.g., vaccine). This may lead to more effective strategies for preventing the rapid transmission of seasonal influenza and contribute to decision-making in infection control and public health.

INTRODUCTION

Seasonal influenza is a respiratory infectious disease caused by the influenza virus, which is associated with significant morbidity and mortality and poses a great threat to public health. In Japan, the annual prevalence of seasonal influenza is >10%.[1] Considering its extensive effect on the community, the National Epidemiological Surveillance of Infectious Diseases (NESID) program (under Infectious Disease Control Law executed in 1999) listed seasonal influenza as a target illness.[2] Moreover, specific medical facilities (termed *influenza sentinel sites*) are required to report the weekly number of cases to the public health center. The weekly sentinel surveillance data are based on medically attended influenza cases, mostly diagnosed microbiologically through a rapid influenza diagnostic test (RIDT).

The sentinel surveillance data for influenza (free-access, real-world surveillance data) are widely available worldwide.[3–5] Previous studies developed risk assessment models using these epidemiological surveillance data. The models were mainly focused on the (1) prediction of future influenza activity and (2) evaluation of the effect of preventive measures (e.g., respiratory protective device, handwashing, social distancing, and vaccination) and treatment interventions (e.g., antiviral treatment). Stochastic (probabilistic) and deterministic (compartmental) models are the most common epidemiological modeling techniques.[6] Deterministic models have been widely used for the construction of respiratory disease transmission models; the susceptible-infected-removed (SIR) and susceptible-exposed-infected-removed models are the most notable.[7,8] This SIR model has also been extensively in physical sciences literature to explain influenza dynamics[9–11] by coupling the changes in the population of susceptible (S), the population of infection cases (I), and the population of recovery to an immune state (R).[12] Although numerous previous studies investigated the transmission and prevention of influenza using the SIR and related models, a major knowledge gap remains with regard to the effect of preventive measures and treatment interventions.[13–15]

The World Health Organization recommends vaccination against seasonal influenza as the most effective approach to preventing infection and severe outcomes caused by the virus.[16] However, the effect of vaccination varies between age groups. In 2019, the Centers for Disease Control and Prevention (CDC) conducted a meta-analysis of the 2018/2019 season data, when the strain had been predicted accurately a priori. The results showed that vaccination against influenza was effective in preventing medically attended, laboratory-confirmed infection in 60% (95% confidence interval [CI], 43%–71%) of children aged <17 years compared with 37% (95% CI, 9%–56%) and 24% (95% CI, −15% to 51%) in those aged 18–49 and ≥50 years, respectively.[17]

Most developed countries have implemented vaccination policies for seasonal influenza, targeting older individuals and those at higher risk of disease.[18] However, the epidemics of influenza in the total population may be mainly driven by children; consequently, the United Kingdom introduced universal vaccination for children since 2013.[19–24]

Considering the experience and observations noted thus far, a quantitative evaluation of the effect of vaccination against influenza with a particular focus on age is urgently warranted. Interpreting the incidence data of medically attended influenza with respect to the weekly time course is analogous to the nature of data on the dose concentration–effect relationship in clinical

pharmacology. In addition, the SIR and related models can be quantitatively revised using pharmacometric modeling techniques. In this study, we incorporated a pharmacometric approach using the SIR framework to create a novel SIR plus vaccination (SIR + V) model for Tokyo, Japan, based on the sentinel surveillance data collected by the NESID. The parameters of the developed model were related to the basic reproductive number (R_0), a widely accepted measure of transmissibility of the virus, for each influenza season.[25] Using this model, we evaluated the efficacy of vaccination against seasonal influenza using local epidemiological and virological data, focusing on the effect of age.

METHODS

Symptomatic influenza population surveillance and virological data

In Japan, the Infectious Disease Surveillance Center of the National Institute of Infectious Diseases (NIID) is notified by prefectural public health institutes regarding the number of cases of infectious diseases. The number of patients diagnosed with symptomatic influenza population (SIP) is determined on a weekly basis from >400 sentinel sites in Tokyo. The data are aggregated by means of SIP cases per sentinel (CPS) population diagnosed with RIDT at the NIID into the weekly total number based on the national and prefectural numbers of cases.[26] The surveillance data are published on the website of the Infectious Disease Weekly Report.[1] In Japan, the aggregated SIP CPS data comprise cases mostly diagnosed microbiologically using a RIDT. The SIP CPS are the combined data of multiple influenza virus strains diagnosed with RIDT with a sensitivity of 73%–86% and a specificity of 97%–100%[27]; thus, the SIP CPS numbers are an appropriate proxy for the total number of symptomatic influenza cases.

In this study, the influenza season ranged from week 36 in September each year up to week 35 in August of the following year according to the structure of data in the NESID. Considering the importance of the pandemic influenza A H_1N_1/09 virus (type A/H_1pdm09) strain discovered in 2009, data obtained before 2009 were excluded from the analysis.[28] Moreover, data collected after 2019 were also excluded because of the extraordinary decrease in the influenza epidemic influenced by the concurrent COVID-19 pandemic, which arose in January 2020, complicating the mathematical modeling.[29] Therefore, we used the SIP CPS data from week 36 of 2010 to week 35 of 2019, covering a total of 10 influenza seasons (Figure S1). The NIID also reports virological test results weekly as well as the absolute number and types of influenza strains.[30] These data were used to estimate the prevalence of each strain per season.

Age-stratified data collection for virus strain population and viral antibody positivity

For each of the 10 seasons of the study, age-stratified data of influenza virus strains and the fraction of H_1 antibody positivity were obtained from the NIID data set.[30,31] Using these data, we were able to determine the isolated influenza virus strain proportion per season (VirusFrac)[30] and age-stratified proportion of seropositive H_1 antibody titer per influenza virus strain per season (PositiveAb).[31] We considered four age groups accordingly to compare the age group representation in the *Morbidity and Mortality Weekly Report* (*MMWR*) from the CDC[17]: infants (≤4 years), children and adolescents (5–14 years), adults (15–69 years), and elderly adults (≥70 years) (Figure S2). The *MMWR* data used to calculate the vaccination effect were separated into the following three groups: 6 months–14 years, 15–49 years, and 50 years and older. The Japanese surveillance data in the NIID are composed of 5-year increments until age 20 and 10-year increments until age 70, and the rest are summed as 70 years and older. The pediatric populations were divided to focus on the differences of social relationship dependence, and the elderly adult population was represented by the 70 years and older group as a pure elderly age population in a longevity country.

Pharmacometric modeling for SIP CPS

The pharmacometric model applied to the present study aimed to calculate the change in SIP CPS over time using the following pharmacometric model:

$$\frac{dA(t)}{dt} = -K_{in} \times A(t)$$

$$\frac{dB(t)}{dt} = K_{in} \times A(t) - K_{out} \times B(t)$$

$$K_{in} = \text{Slope} \times B(t)$$

$A(t)$ accounts for the patients potentially becoming SIP CPS (i.e., potential SIP CPS [PSIP CPS]) and $B(t)$ is equivalent to SIP CPS. K_{in} (1/week) accounts for the transmission rate from $A(t)$ to $B(t)$ and is dependent on $B(t)$. K_{out} (1/week) defines the elimination of $B(t)$. To set the initial condition in the $dB(t)/dt$ equation, we assumed that at the

beginning of the epidemic, a small fraction of individuals in each age group were in *B(t)*, whereas the remaining individuals were in *A(t)*. Therefore, the very beginning of *A(t)* is initialized to "A_0" and after *Tlag* (week), which is the interval time until the onset of the epidemic. *B(t)* is initialized to "Baseline," where "A_0" is estimated from the data and "Baseline" was arbitrarily fixed to the lowest possible measured value, which was 0.01 in this study. A_0, *Slope*, and *Tlag* were unknown parameters to be estimated. The random effects of inter-seasonal variability on A_0, *Slope*, and *Tlag* were described using an exponential error model.

Because the fundamental model structure is equivalent to that of the SIR model, we tested three different residual error models (i.e., additive, proportional, and combined additive–proportional) as a base structural model. Model selection was guided by plausible parameter estimates, precision of the parameters, visual diagnostics, and the minimum objective function value (OFV) calculated as proportional to minus twice the log-likelihood. A reduction in OFV ≥3.84 denoted significant improvement ($p < 0.05$) in model description. Based on the significant and lowest OFV value, as well as adequate model parameters and visual diagnostics, the indirect response model equivalent to the SIR model with the combined additive–proportional error model was selected as the most appropriate structure.

Determination of the covariate model to determine the virus strain and effect of vaccination

Clinical factors were screened as potential covariates that could affect SIP CPS using a stepwise covariate modeling approach with forward selection ($p < 0.05$) and backward elimination ($p < 0.01$). Potential factors were the fractions of isolated influenza virus strain per season (VirusFrac_i) and seropositive H_1 antibody titer per influenza virus strain (PositiveAb_i). Influenza virus strains are divided into four major types (types A to D) and types A and B are the major influenza virus types that cause seasonal epidemic of the disease. Influenza A virus is subdivided based on the following two proteins on the surface of the virus: hemagglutinin (HA) and neuraminidase (NA). Although there are potentially 198 different influenza A subtype combinations, viruses that routinely circulate are A/H_1pdm09 and A/H_3N_2. Influenza B is not divided into subtypes but classified into the following two lineages: B/Victoria and B/Yamagata. Therefore, we chose four major strains ($i = 1$: A/H_1pdm09; $i = 2$: A/H_3N_2; $i = 3$: B/Victoria; $i = 4$: B/Yamagata) as the circulating strains included in the study in the 10 influenza seasons in Japan.

Because the vaccine against seasonal influenza is not completely effective, only a proportion of the vaccinated population was assumed to be protected. We assumed that the effect of vaccination on each circulating strain can be described as multiplication of VirusFrac_i and PositiveAb_i with an exponent of θvirus_i for each strain. We defined a new parameter as follows:

$$\text{Preventive effect} = \sum_1^4 (\text{VirusFrac}_i \times (1 - \text{PositiveAb}_i))^{\theta_{\text{virusi}}},$$

where VirusFrac_i represents the proportion of the *i*-th type of virus found in each influenza season ($\sum_1^4 \text{VirusFrac}_i = 1$), PositiveAb_i represents the proportion of seropositive H_1 antibody titer for the *i*-th type of virus ($0 \le \text{PositiveAb}_i \le 1$), and θvirus_i accounts for the effect of vaccination against the *i*-th type of the virus.

To assess the preventive effect of vaccination, we investigated two models from the possible mechanism of action: the preventive inhibitory effect on K_{in} and the stimulated recovery effect on K_{out}. The preventive inhibitory effect on K_{in} is self-explanatory from the nature of the vaccine to prevent from infection. Concerning the stimulated recovery effect on K_{out}, a recent study explained the mechanism of B cell immune response induction with influenza vaccination through HA, NA, and M2 protein upregulation.[32] B cell immune response stimulates apoptosis of infected cells, which results in decreasing the influenza symptomatic patient number. This is equivalent to the stimulated recovery effect on K_{out}.

Univariate analysis revealed that both models were statistically significant, and the preventive inhibitory effect model was superior to the stimulated recovery effect model. However, when both effects were simultaneously implemented in the model, the model did not reach statistical significance compared with the preventive inhibitory effect model alone. Therefore, we selected the preventive inhibitory effect model to describe the preventive effect. The following is the final model (Figure 1):

$$\frac{dA(t)}{dt} = -K_{\text{in}} \times A(t)$$

$$\frac{dB(t)}{dt} = K_{\text{in}} \times A(t) - K_{\text{out}} \times B(t)$$

$$K_{\text{in}} = \text{Slope} \times B(t) \times \text{Preventive effect}$$

$$\text{Preventive effect} = \left\{ \begin{array}{l} (\text{VirusFrac}_1 \times (1 - \text{PositiveAb}_1))^{\theta_{\text{virus1}}} \\ + (\text{VirusFrac}_2 \times (1 - \text{PositiveAb}_2))^{\theta_{\text{virus2}}} \\ + (\text{VirusFrac}_3 \times (1 - \text{PositiveAb}_3))^{\theta_{\text{virus3}}} \\ + (\text{VirusFrac}_4 \times (1 - \text{PositiveAb}_4))^{\theta_{\text{virus4}}} \end{array} \right\}$$

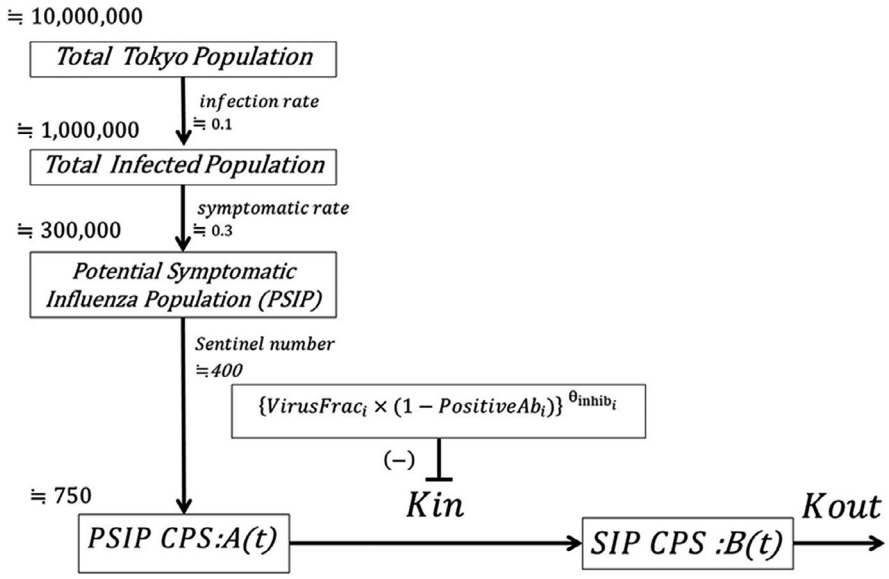

FIGURE 1 The modeling diagram of the spread of influenza in Tokyo, Japan, and the effect of vaccination on the spread of patients with symptomatic influenza. Final model: $\frac{dA(t)}{dt} = -K_{in} \times A(t)$, $\frac{dB(t)}{dt} = K_{in} \times A(t) - K_{out} \times B(t)$, $K_{in} = \text{Slope} \times B(t) \times \text{Preventive effect}$,

$$\text{Preventive effect} = \left\{ \begin{array}{l} \left(\text{VirusFrac}_1 \times (1 - \text{PositiveAb}_1)\right)^{\theta_{\text{virus1}}} \\ + \left(\text{VirusFrac}_2 \times (1 - \text{PositiveAb}_2)\right)^{\theta_{\text{virus2}}} \\ + \left(\text{VirusFrac}_3 \times (1 - \text{PositiveAb}_3)\right)^{\theta_{\text{virus3}}} \\ + \left(\text{VirusFrac}_4 \times (1 - \text{PositiveAb}_4)\right)^{\theta_{\text{virus4}}} \end{array} \right\}, \text{Slope} \geq 0, \sum_1^4 \text{VirusFrac}_i = 1, 0 \leq \text{PositiveAb}_i \leq 1.$$

$A(t)$ denotes potential symptomatic influenza population cases per sentinel (PSIP CPS; patients with a positive rapid influenza diagnostic test [RIDT] without any symptoms). $B(t)$ denotes symptomatic influenza population cases per sentinel (SIP CPS). VirusFrac_i denotes the fraction of the i-th virus. K_{in} denotes the transmission rate from $A(t)$ to $B(t)$. K_{out} denotes the elimination rate of $B(t)$. PositiveAb_i denotes the fraction of the positive antibody titer in i-th virus. θ_{inhib_i} denotes the inhibitory effect caused by flu vaccination on the i-th virus. In Japan, the cumulative infection rate in the total population is approximately 10%.[2] This population is defined as the total infected population. Seasonal influenza results in asymptomatic and subclinical (i.e., with symptoms not diagnostic for influenza, such as being afebrile) infection with moderately high probability. There is approximately 30% chance for those who actually consult a doctor to have a positive RIDT.[41] This population is defined as the potential symptomatic influenza population (PSIP). This population was divided into sentinel in Tokyo (PSIP CPS $A(t)$). In this model, PSIP CPS and SIP CPS were connected with a rate constant K_{in}. Following the recovery of a patient, we assume that the person will remain immune (i.e., will not return back to $A(t)$ or $B(t)$) for the rest of that influenza season). The $B(t)$ represents observed (dependent) values obtained from the original National Epidemiological Surveillance of Infectious Diseases data set. In addition to this structural model, we assumed that the preventive effect for each circulating strain can be written as multiplication of the fraction of the i-th virus (VirusFrac_i) and fraction of positive antibody titer in the i-th virus (PositiveAb_i), with the inhibitory effect caused by vaccination against influenza (θ_{inhib}) as an exponent

$$\text{Slope} \geq 0\,, \sum_1^4 \text{VirusFrac}_i = 1, 0 \leq \text{PositiveAb}_i \leq 1$$

Because $\text{VirusFrac}_i \times (1 - \text{PositiveAb}_i)$ is in the range of zero to unity, and θvirus_i indicates the inhibitory effect exerted by vaccination on K_{in}. We compared the estimates of θvirus_i to quantitatively evaluate the effect on each virus strain.

Model evaluation

Goodness-of-fit plots were used to evaluate the model. The stability and performance of the final model was investigated by a nonparametric bootstrap analysis. The final model was refitted to each of the randomly sampled replicates of the original data one at a time; this process was repeated 500 times with different random draws. The means, standard errors, and 95% confidence intervals (CIs) for the parameters were obtained. The model was further validated using an external data set of a different prefecture in Japan (Hokkaido) and the parameter estimates obtained by the data obtained in Tokyo.

Susceptibility according to age

The estimation of differences in susceptibility based on the age was conducted by calculating parameters shown for each age group. Differences in K_{in} observed in various age groups represent the variability in the likelihood of influenza infection among the corresponding age groups. Hence, a higher K_{in} value indicates larger relative

impact on the basic reproduction number (R_0) of the epidemic,[33,34] corresponding to the peak incidence in the community.

Calculation of prevention factor

We defined the preventive effect as the following:

$$\text{Preventive effect} = \left\{ \begin{array}{l} \left(\text{VirusFrac}_1 \times (1 - \text{PositiveAb}_1)\right)^{\theta_{\text{virus1}}} \\ + \left(\text{VirusFrac}_2 \times (1 - \text{PositiveAb}_2)\right)^{\theta_{\text{virus2}}} \\ + \left(\text{VirusFrac}_3 \times (1 - \text{PositiveAb}_3)\right)^{\theta_{\text{virus3}}} \\ + \left(\text{VirusFrac}_4 \times (1 - \text{PositiveAb}_4)\right)^{\theta_{\text{virus4}}} \end{array} \right\}$$

There are four different virus subtypes in the source data. Thus, we calculated the preventive effect against each of those subtypes in the following two scenarios: (1) PositiveAb_i was substituted by 1 assuming 100% antibody titer positivity in the allotted i-th virus subtype (Scenario A_i) and (2) PositiveAb_i was substituted by 0, assuming 0% antibody titer positivity in the allotted virus subtype (Scenario B_i). Subsequently, using the preventive effect, we further defined the prevention factor for the i-th virus subtype in the following:

$$\text{Prevention factor} = 100\,\% \times \left(1 - \frac{\text{Preventive effect in Scenario } A_i}{\text{Preventive effect in Scenario } B_i}\right)$$

The four different scenarios for calculation were as follows:

100% antibody titer positivity for the A/H_1pdm09 strain ($\text{PositiveAb}_1 = 1$). (Versus Scenario B_1: $\text{PositiveAb}_1 = 0$)

100% antibody titer positivity for the A/H_3N_2 strain ($\text{PositiveAb}_2 = 1$). (Versus Scenario B_2: $\text{PositiveAb}_2 = 0$)

100% antibody titer positivity for the B/Victoria strain ($\text{PositiveAb}_3 = 1$). (Versus Scenario B_3: $\text{PositiveAb}_3 = 0$)

100% antibody titer positivity for the B/Yamagata strain ($\text{PositiveAb}_4 = 1$). (Versus Scenario B_4: $\text{PositiveAb}_4 = 0$)

Of note, in the calculation of the preventive effect for the i-th virus subtype, the other $PositiveAb_j$ values for the j-th subtype ($j \neq i$), were fixed to the estimated values. Calculation of the prevention factor for each subtype allowed us to estimate the relative inhibitory effect of vaccination, which prevented infection by each strain during the influenza epidemics. The same calculation was performed for different age groups to estimate the age-dependent inhibitory effect of the vaccination against the A/H_1pdm09 strain.

R_0 estimation

The R_0 in the SIR model is described as follows[16]:

$$R_0 = \frac{\beta N}{\gamma}$$

N accounts for the total influenza-susceptible population, β defines the disease transmission rate constant, and $1/\gamma$ denotes the mean infectious period; $\gamma > 0$ is the recovery rate.[35] Typically, R_0 is a threshold value determining the potency of the disease. The mean R_0 of seasonal influenza in three countries (United States, France, and Australia) was 1.3 (range, 0.9–2.1),[36] whereas the R_0 range for the 2009 H_1N_1 influenza infection in Japan was 2.0–2.4.[37] The present pharmacometric model is related to the original SIR model, and both parameters can be associated as follows:

$$\beta = \text{Slope}$$

$$\beta I(t) = K_{\text{in}} \cdots \text{transmission of influenza infection}$$

$$N = A_0$$

$$\gamma = K_{\text{out}}$$

Therefore, the R_0 can be expressed using the following formula:

$$R_0 = \frac{\text{Slope} \times A_0}{K_{\text{out}}}$$

We calculated the R_0 using this equation and the obtained parameter estimates.

Software

The pharmacometric analysis for SIP CPS was performed using the Phoenix NLME software Version 8.1 (Certara) with a Hewlett-Packard Z640 workstation (Intel Xeon E5 processor, 2.60 GHz, 28 cores). The First-Order Conditional Estimation Extended Least Squares computational algorithm was used.

RESULTS

Evaluation of the final model

Table 1 summarizes the characteristics of seasonal influenza epidemics from 2010/2011 to 2018/2019, estimated using the present pharmacometric model. The

TABLE 1 Parameter estimates from the SIR + V model

Parameter (units)	Estimate	Bootstrap			Shrinkage
		Mean	SE	95% CI (2.5th percentile, 97.5th percentile)	
θK_{out} (/week)	0.1786	0.1789	0.02180	0.1239, 0.2256	
$\theta Tlag$ (week)	16.51	16.06	2.305	9.854, 20.12	
$\theta \text{Virus}_{\text{A/H1pdm09}}$	1.794	1.815	0.1168	1.594, 2.100	
$\theta \text{Virus}_{\text{A/H3N2}}$	1.797	1.821	0.1389	1.533, 2.132	
$\theta \text{Virus}_{\text{B/Victoria}}$	1.921	1.939	0.1349	1.657, 2.216	
$\theta \text{Virus}_{\text{B/Yamagata}}$	1.917	1.935	0.1348	1.672, 2.272	
θA_0 (PSIP CPS baseline)	540.91	558.86	86.94	412.52, 794.60	
θSlope	0.5475	0.5659	0.07983	0.4208, 0.7855	
σprop	0.6244	0.5379	0.1188	0.3207, 0.7450	
σadd	0.1317	0.1244	0.01517	0.08560, 0.1490	
$\omega^2 K_{out}$	9.291	9.460	1.131		0.6919
$\omega^2 Tlag$	11.30	11.46	1.363		0.7683
$\omega^2 \theta \text{Virus}_{\text{A/H1pdm09}}$	4.401	4.513	0.5658		0.8647
$\omega^2 \theta \text{Virus}_{\text{A/H3N2}}$	4.364	4.466	0.5546		0.8515
$\omega^2 A_0$	10.65	10.89	1.370		0.5707
$\omega^2 Slope$	9.145	9.395	1.272		0.8207

Note: Final model: $\frac{dA(t)}{dt} = -K_{in} \times A(t)$, $\frac{dB(t)}{dt} = K_{in} \times A(t) - K_{out} \times B(t)$

$K_{in} = \text{Slope} \times B(t) \times \text{Preventive effect}$

$$\text{Preventive effect} = \left\{ \begin{array}{l} \left(\text{VirusFrac}_1 \times (1 - \text{PositiveAb}_1)\right)^{\theta_{\text{virus1}}} \\ + \left(\text{VirusFrac}_2 \times (1 - \text{PositiveAb}_2)\right)^{\theta_{\text{virus2}}} \\ + \left(\text{VirusFrac}_3 \times (1 - \text{PositiveAb}_3)\right)^{\theta_{\text{virus3}}} \\ + \left(\text{VirusFrac}_4 \times (1 - \text{PositiveAb}_4)\right)^{\theta_{\text{virus4}}} \end{array} \right\}$$

$\sum_1^4 \text{VirusFrac}_i = 1, \text{Slope} \geq 0, 0 \leq \text{PositiveAb}_i \leq 1$

Abbreviations: A/H_1pdm09, pandemic influenza A H_1N_1/09 virus; A/H_3N_2, influenza A H_3N_2 virus; *A(t)*, PSIP CPS according to time; baseline, the beginning of *B(t)*; *B(t)*, Symptomatic Influenza Patients Cases Per Sentinel (SIP CPS) according to time; CI, confidence interval; K_{in} (1/week), the spreading rate from *A(t)* to *B(t)* and is dependent on *B(t)*; K_{out} (1/week), the elimination of *B(t)*; PositiveAb_i, the proportion of seropositive H_1 antibody titer for the *i*-th ($i = 1,2,3,4$) type of virus ($0 \leq \text{PositiveAb}_i \leq 1$); PSIP CPS, Potential Symptomatic Influenza Patients Case Per Sentinel (patients with a positive rapid influenza diagnostic test [RIDT] without any symptoms); SIR+V, Susceptible-Infected-Removed plus Vaccination; Slope, coefficient of K_{in}; *Tlag* (week), interval till the epidemic onset; VirusFrac_i, the proportion of the *i*-th ($i = 1$: A/H_1pdm09, $i = 2$: A/H_3N_2, $i = 3$: B/Victoria, $i = 4$:B/Yamagata, respectively) type of virus found in each influenza season ($\sum_1^4 \text{VirusFrac}_i = 1$); θvirus_i, the inhibitory effect caused by flu vaccination for the *i*-th ($i = 1,2,3,4$) type of virus; ω^2, omega squared (variance); σ, sigma (standard deviation); σprop, σadd, standard deviations of proportional and additive error of the combined intraindividual error model, respectively.

The *B(t)* represents observed (dependent) values obtained from the original National Epidemiological Surveillance of Infectious Diseases data set.

developed model accurately reproduced the detailed epidemiological patterns of observed surveillance data, and the model fitting was confirmed by goodness-of-fit plots (Figure S3). The stability and robustness of the obtained parameters were confirmed using a bootstrap method. A total of 486/500 bootstrap runs reached successful convergence, and the ratios of the bootstrap mean/final estimate were within an acceptable range (Table 1). The estimated mean of *Tlag* (week) was 16.51 weeks, and the standard deviation for the interseasonal variability of *Tlag* ($\omega Tlag$) was 3.36 weeks. The interseasonal variability of *Tlag* indicated that the onset of each of the influenza seasons differed annually, rendering the uniform comparison between prediction and observation for all seasons challenging. Therefore, individual prediction and individual weighted residuals were selected for comparison (Figure S3).

Across 10 seasons, it was estimated that the baseline PSIP CPS was 540.9 ($= A_0$), which was slightly lower than that expected from the estimation in Figure 1. The estimated interval until the onset of the epidemic was 16.51 weeks. This was compatible with the previously reported onset of the epidemic (mean, 15.2 weeks) based on the empirical threshold method. According to this method, a weekly number of influenza-like illness CPS exceeding the prespecified threshold of 1.0 for 3 consecutive weeks denotes an epidemic.[38]

The same model and parameter estimates shown in Table 1 were used to predict the SIP CPS of Hokkaido, Japan, as an external evaluation. The goodness-of-fit plots (Figure S4) showed good agreement with the observed SIP CPS data set.

Virus strain effect

The $\theta virus_i$ values of the five virus strains were similar (1.794–1.921) (Table 1). However, when the final model was compared with the model assuming commonly shared $\theta virus_i$ value, the difference of OFV was 12.87. This accounted for $p = 0.012$ and resulted in significantly different $\theta virus_i$ values in the final model. A significant difference in $\theta virus_i$ value of 1.794 (A/H_1pdm09: preventive effect, 0.169) and 1.921 (B/Victoria: preventive effect, 0.144) was observed, which accounted for 0.025 difference in the preventive effect (0.169 and 0.144 for A/H_1pdm09 and B/Victoria, respectively). Therefore, slight significance was observed in the effect of different virus strains on K_{in}; however, the magnitude of the effect was minimal.

Susceptibility according to age

Figure 2 provides the estimated K_{in} for four age groups (≤4 years, 5–14 years, 15–69 years, and ≥70 years) for 10 influenza season epidemics. We have performed a parametric normal test (Z test) between the highest K_{in} estimate group (5–14 years) and the second highest K_{in} estimate group (≤4 years) using mean/standard error (SE). The p value of the Z test was <0.001, and therefore children aged 5–14 years showed the highest estimates of K_{in} among all age groups. Thus, this age group may be susceptible to influenza infection, causing a large increase in SIP CPS in the whole population.

Preventive efficacy of vaccination among different virus strains and age groups

Prevention factor of vaccination for four virus strains and different age groups were calculated (Tables 2 and 3). The highest and lowest values of the prevention factor were noted for influenza type A/H_3N_2 strain (82.7%, Table 2) and type B/Victoria strain (6.3%, Table 2), respectively. Within the A/H_1pdm09 strain, the largest and smallest impact were observed in groups aged 5–14 years (70.8%) and 0–4 years (41.8%), respectively (Table 3).

Calculation of the R_0

Table 4 presents the results of the R_0 calculation. The calculated values for R_0 ranged 1.29–3.87, indicating a $R_0 > 1$ in all previous 10 influenza seasons. The average R_0 was 2.12 ± 0.95, which was trending higher than those observed in three countries (United States, France, and Australia), with a mean value of 1.3 (range, 0.9–2.1).[36]

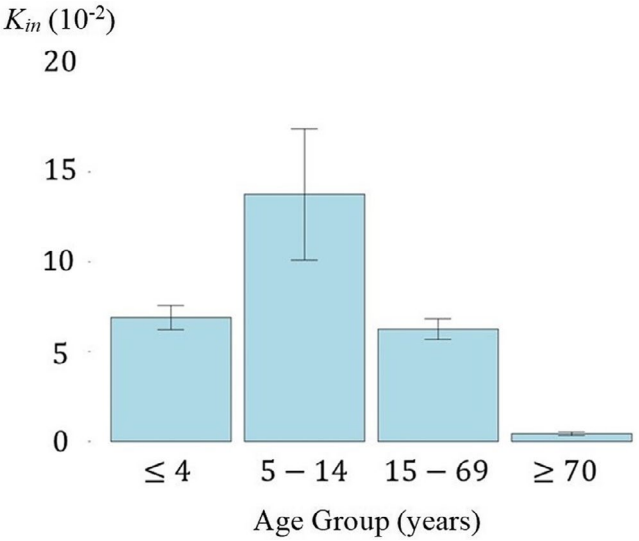

FIGURE 2 Estimate of the K_{in} mean for various age groups. The graph represents the mean K_{in} value of the population estimate in 10 influenza seasons (i.e., from 2010 to 2019) with its standard deviation. For epidemics associated with influenza A and B in total, children aged 5–14 years had the highest estimates of K_{in} among all age groups for the 10 influenza season epidemics. K_{in}, a parameter describing the transmission rate of symptomatic influenza infection

TABLE 2 Prevention factor according to antibody positivity per virus strain

Virus type	0% Antibody titer (Scenario B) Preventive effect[a] Mean	SD	100% Antibody titer (Scenario A) Preventive effect[a] Mean	SD	Prevention factor[b]
A/H_1pdm09	0.272	0.144	0.119	0.088	56.1
A/H_3N_2	0.389	0.186	0.067	0.072	82.7
B/Victoria	0.176	0.075	0.165	0.074	6.3
B/Yamagata	0.198	0.065	0.156	0.080	21.0

[a] Preventive effect $= \sum_{i=1}^{4} \left\{ \text{VirusFrac}_i \times (1 - \text{PositiveAb}_i) \right\}^{\theta_{virus_i}}$.

[b] $\text{Prevention factor}(\%) = \left(1 - \frac{\text{Prevention effect 100\% (Scenario A)}}{\text{Prevention effect 0\% (Scenario B)}}\right) \times 100$.

TABLE 3 Prevention factor according to different age groups for influenza type A/H_1pdm09

A/H_1pdm09	0% Antibody titer (Scenario B)		100% Antibody titer (Scenario A)		
	Preventive effect[a]		Preventive effect[a]		Prevention factor[b]
Age group, years	Mean	SD	Mean	SD	
≤4	0.365	0.113	0.213	0.130	41.8
5–14	0.216	0.171	0.0629	0.0542	70.8
15–69	0.274	0.143	0.121	0.0931	55.8
≥70	0.289	0.150	0.136	0.116	52.9

[a]Preventive effect $= \sum_{i=1}^{4} \left\{\text{VirusFrac}_i \times \left(1 - \text{PositiveAb}_i\right)\right\}^{\theta_{\text{virus}i}}$.

[b]Prevention factor$(\%) = \left(1 - \frac{\text{Preventive effect 100\% (Scenario A)}}{\text{Preventive effect 0\% (Scenario B)}}\right) \times 100$.

TABLE 4 Seasonal estimation of basic reproduction number R_0

Seasons	R_0
2010–2011	1.29
2011–2012	2.09
2012–2013	3.87
2013–2014	1.32
2014–2015	3.57
2015–2016	1.64
2016–2017	1.35
2017–2018	1.39
2018–2019	2.56
Average ± SD	2.12 ± 0.95

Note: $R_0 = \frac{\text{Slope} \times A_0}{K_{\text{out}}}$

Abbreviation: A_0, Potential Symptomatic Influenza Population Cases Per Sentinel (PSIP CPS) baseline; K_{out}, the elimination rate of $B(t)$ (Symptomatic Influenza Population Cases Per Sentinel (SIP CPS)); R_0, basic reproduction number.

Nevertheless, it was highly compatible with the previously calculated R_0 values for H_1N_1 seasonal influenza infection in Japan (range, 2.0–2.4).

DISCUSSION

In this study, a newly developed mathematical SIR + V model successfully described the patterns of influenza epidemics in addition to the quantification of the efficacy of vaccination among different virus strains and age groups. This is the first model to achieve this objective. The model-based simulations in designated strains and age groups identified the most influential group for the transmission of influenza. Furthermore, we newly derived converting formulas between our parameters (K_{out}, A_0, and β) and traditional index (R_0) for each influenza season. The calculation using our parameters matched the actual R_0 values.

The relative impact of different age groups on influenza epidemics was not fully elucidated. Furthermore, there is no clear understanding of the importance of age in the transmission of influenza virus and the mechanism through which vaccination may compensate for this influence. A previous study[22] suggested that children aged 5–17 years were at the highest relative risk for an influenza A outbreak in the United States. Because K_{in} is rewritten as $\beta I(t)$, which is equivalent to the transmission of infection in the SIR model, the relative changes in K_{in} in the present model and the prevention factor could reliably identify the age group and the key viral strain that plays the most important relative role in transmission during a particular epidemic. A key utility of K_{in} lies in the fact that it can be readily estimated from appropriate epidemic data (in our case, SIP CPS data) serving as a surrogate measure for age-specific differences in the incidence of influenza epidemics.

Moreover, even if groups differ in the proportion of incident cases of influenza infection and viral strain fractions, the ordering of groups by K_{in} and prevention factor reflects the ordering of the proportional change in the incidence of infection in these groups.

The present analysis indicates that for the past 10 influenza seasons, children and adolescents aged 5–14 years and elderly individuals aged ≥70 years had the highest and lowest K_{in} value, respectively. Although the data set did not provide insight into living environments, such as schools, this result is consistent with the notion supported by several studies.[22,39,40] Therefore, children and adolescents are most susceptible to influenza infection in the whole community.

Tables 2 and 3 show the estimated prevention factors of vaccination for four virus strains and different age groups. The findings revealed that the current vaccine is more effective against influenza type A. This is because type A was the dominant fraction of influenza virus for the past 10 seasons. In the 2018–2019 *MMWR* published by the CDC, the estimated fraction of prevention of

positivity for A/H_1pdm09 and A/H_3N_2 among the vaccinated population was 46% (95% CI, 30%–58%) and 44% (95% CI, 13%–64%), respectively. Information concerning the percentages of the vaccinated population and positive RIDT among patients who are symptomatic is essential to accurately calculate the efficacy of vaccination, as in the *MMWR*. However, by implementing the SIR + V model together with a new parameter, prevention factor, we were able to calculate the magnitude of the vaccination effect without requiring actual percentage data.

We sought to explore the role of a higher value of K_{in} in the SIP CPS data as a driver of influenza epidemics for a particular age group. We also attempted to determine the potential impact of increased vaccination efforts in a group with a high K_{in} on the dynamics of influenza transmission in the population. For this purpose, we evaluated antibody titer positivity among different age groups. We found that, for epidemics associated with influenza A/H_1pdm09, the group with the highest K_{in} value in the data also showed the highest prevention factor (Table 3, Figure 2). However, this correlation was not observed in the elderly possibly because of the relative high fraction of antibody positivity for the A/H_1pdm09 virus.

It is uncertain to what extent the proposed simulation framework reflects the reality of influenza transmission in the community. Our primary aims using the simulation were to (1) examine the effect of vaccination against influenza on each viral strain, (2) investigate whether vaccination would be most effective in age groups with the highest K_{in} values, and (3) assume the relative effect size of the vaccination against influenza. The calculated value of the prevention factor depends on the fraction of each virus strain and the seropositivity data against influenza virus strains from the previous year. Therefore, the prevention factor does not always indicate absolute values of actual efficacy. Because of the lack of direct comparison data of influenza infection between vaccinated and unvaccinated populations, such as the *MMWR* from the CDC, similar types of data are strongly warranted to ensure direct comparisons of the efficacy of vaccination.[17]

The present method has some additional limitations. The model was based on single peaked influenza infection data. The 2019/2020 influenza SIP CPS graph in Japan showed two-peak observation data. The same multiple peak phenomena were also observed in other countries such as the United States, Canada, and Australia. In the 2019/2020 season, the precedent influenza infection began with type AH_1pdm09 infection followed by type B Victoria infection in many counties. The concurrent circulation of multiple subtypes of seasonal influenza infection possibly resulted in multiple peak infection. The current model is unable to describe the two-peak trends and requires further refinement. Moreover, we have fixed the baseline initial transmission dynamic phase value to 0.01, the lowest measurable SIP CPS value, instead of estimating by an ordinary least squares method. This assumption of baseline initial transmission value did not alter the accuracy to evaluate the vaccination effect for each viral strain.

Despite these limitations, this analysis provides insight into the dynamics of cross-seasonal influenza infection using the novel SIR + V model. The proposed model and simulation results revealed variability in the effect of vaccination among different virus strains and age groups during influenza epidemics. The present results indicate a critical role of vaccination to school-age children for the effective prevention of influenza transmission.

ACKNOWLEDGMENT

We thank Enago (www.enago.co.jp) for assistance with language editing in this article.

CONFLICT OF INTEREST

The authors declared no competing interests for this work.

AUTHOR CONTRIBUTIONS

Y.O., H.K., and Y.T. wrote the manuscript. Y.O. and Y.T. designed the research. Y.O., H.K., and Y.T. performed the research. Y.O., H.K., and Y.T. analyzed the data.

REFERENCES

1. National Institute of Infectious Diseases Japan. Influenza (in Japanese). https://www.niid.go.jp/niid/ja/diseases/a/flu.html. Published 2020. Accessed March 17, 2021.
2. Taniguchi K, Hashimoto S, Kawado M, et al. Overview of infectious disease surveillance system in Japan, 1999–2005. *J Epidemiol*. 2007;17(suppl):S3-13.
3. World Health Organization (WHO), *FluNet*. https://www.who.int/influenza/gisrs_laboratory/flunet/en/. Published 2021. Accessed March 17, 2021.
4. Yale School of Public Health. *FluSurv-NET-Influenza and RSV Surveillance*. https://ysph.yale.edu/eip/projects/flu/. Published 2020. Accessed March 17, 2021.
5. Centers for Disease Control and Prevention (CDC). *Weekly U.S. Influenza Surveillance Report (FluView)*. https://www.cdc.gov/flu/weekly/index.htm. Published 2021. Accessed March 17, 2021.
6. Kendall DG. *Deterministic and stochastic epidemics in closed populations*. Proceedings of the Third Berkeley Symposium on Mathematical Statistics and Probability, Volume 4: Contributions to Biology and Problems of Health. Berkeley, CA: University of California Press; 1956. p. 149-165.
7. Keeling M, Rohani P, Pourbohloul B. Modeling infectious diseases in humans and animals. *Clin Infect Dis*. 2008;47:864-865.
8. Kermack WO, McKendrick AG. A contribution to the mathematical theory of epidemics. *Proc R Soc London Series A*. 1927;115;700-721.
9. O'Regan SM, Kelly TC, Korobeinikov A, O'Callaghan MJA, Pokrovskii AV, Rachinskii D. Chaos in a seasonally perturbed SIR model: avian influenza in a seabird colony as a paradigm. *J Math Biol*. 2013;67:293-327.

10. Diekmann O, Heesterbeek H, Britton T. *Mathematical tools for understanding infectious disease dynamics*. Princeton, NJ: Princeton University Press; 2013.
11. Sambaturu N, Mukherjee S, López-García M, Molina-París C, Menon GI, Chandra N. Role of genetic heterogeneity in determining the epidemiological severity of H1N1 influenza. *PLoS Comput Biol*. 2018;14:e1006069.
12. Stilianakis NI, Drossinos Y. Dynamics of infectious disease transmission by inhalable respiratory droplets. *J R Soc Interface*. 2010;7:1355-1366.
13. Levin SA, Dushoff J, Plotkin JB. Evolution and persistence of influenza A and other diseases. *Math Biosci*. 2004;188:17-28.
14. Laguzet L, Turinici G. Individual vaccination as Nash equilibrium in a SIR model with application to the 2009–2010 influenza A (H1N1) epidemic in France. *Bull Math Biol*. 2015;77:1955-1984.
15. Osthus D, Hickmann KS, Caragea PC, Higdon D, Del Valle SY. Forecasting seasonal influenza with a state-space SIR model. *Ann Appl Stat*. 2017;11:202-224.
16. World Health Organization (WHO). *Influenza (seasonal) fact sheets*. https://www.who.int/news-room/fact-sheets/detail/influenza-(seasonal). Published 2018. Accessed March 17, 2021.
17. Doyle JD, Chung JR, Kim SS, et al. Interim estimates of 2018–19 seasonal influenza vaccine effectiveness—United States, February 2019. *MMWR Morb Mortal Wkly Rep*. 2019;68:135-139.
18. European Center for Disease Prevention and Control. *Vaccine scheduler*. https://vaccine-schedule.ecdc.europa.eu/ Published 2021. Accessed March 17, 2021.
19. Wallinga J, Teunis P, Kretzschmar M. Using data on social contacts to estimate age-specific transmission parameters for respiratory-spread infectious agents. *Am J Epidemiol*. 2006;164:936-944.
20. Basta NE, Chao DL, Halloran ME, Matrajt L, Longini IM Jr. Strategies for pandemic and seasonal influenza vaccination of schoolchildren in the United States. *Am J Epidemiol*. 2009;170:679-686.
21. Reed C, Katz JM, Hancock K, Balish A, Fry AM. Prevalence of seropositivity to pandemic influenza A/H1N1 virus in the United States following the 2009 pandemic. *PLoS One*. 2012;7:e48187.
22. Worby CJ, Chaves SS, Wallinga J, Lipsitch M, Finelli L, Goldstein E. On the relative role of different age groups in influenza epidemics. *Epidemics*. 2015;13:10-16.
23. Cromer D, van Hoek AJ, Jit M, Edmunds WJ, Fleming D, Miller E. The burden of influenza in England by age and clinical risk group: a statistical analysis to inform vaccine policy. *J Infect*. 2014;68:363-371.
24. Baguelin M, Camacho A, Flasche S, Edmunds WJ. Extending the elderly- and risk-group programme of vaccination against seasonal influenza in England and Wales: a cost-effectiveness study. *BMC Med*. 2015;13:236.
25. Heffernan JM, Fau SR, Smith RJ, Wahl LM. Perspectives on the basic reproductive ratio. *J R Soc Interface*. 2005;2:281-293.
26. Zaraket H, Saito R. Japanese surveillance systems and treatment for influenza. *Curr Treat Options Infect Dis*. 2016;8:311-328.
27. Akaishi Y, Matsumoto T, Harada Y, Hirayama Y. Evaluation of the rapid influenza detection tests GOLD SIGN FLU and Quick Navi-Flu for the detection of influenza A and B virus antigens in adults during the influenza season. *Int J Infect Dis*. 2016;52:55-58.
28. Baldo V, Bertoncello C, Cocchio S, et al. The new pandemic influenza A/(H1N1)pdm09 virus: is it really "new"? *J Prev Med Hyg*. 2016;57:E19-E22.
29. Lee H, Lee H, Song K-H, et al. Impact of public health interventions on seasonal influenza activity during the COVID-19 outbreak in Korea. *Clin Infect Dis*. 2021;73(1):e132-e140.
30. National Institute of Infectious Diseases Japan. Isolation/detection of influenza virus in Japan https://www.niid.go.jp/niid/ja/iasr-inf.html Published 2021. Accessed March 17, 2021.
31. National Institute of Infectious Diseases Japan. *National epidemiological surveillance of vaccine-preventable diseases*. https://www.niid.go.jp/niid/en/y-graphs.html Published 2020. Accessed March 17, 2021.
32. Krammer F. The human antibody response to influenza A virus infection and vaccination. *Nat Rev*. 2019;19:383-397.
33. Wallinga J, van Boven M, Lipsitch M. Optimizing infectious disease interventions during an emerging epidemic. *Proc Natl Acad Sci USA*. 2010;107:923.
34. Goldstein E, Apolloni A, Lewis B, et al. Distribution of vaccine/antivirals and the 'least spread line' in a stratified population. *J R Soc Int Royal Soc*. 2009;7:755-764.
35. van den Driessche P. Reproduction numbers of infectious disease models. *Infect Dis Model*. 2017;2:288-303.
36. Chowell G, Miller MA, Viboud C. Seasonal influenza in the United States, France, and Australia: transmission and prospects for control. *Epidemiol Infect*. 2008;136(6):852-864.
37. Nishiura H, Castillo-Chavez C, Safan M, Chowell G. Transmission potential of the new influenza A(H1N1) virus and its age-specificity in Japan. *Euro Surveillance*. 2009;14:19227.
38. Cai J, Zhang B, Xu B, et al. A maximum curvature method for estimating epidemic onset of seasonal influenza in Japan. *BMC Infect Dis*. 2019;19:181.
39. Longini IM Jr. Containing pandemic influenza with antiviral agents. *Am J Epidemiol*. 2004;159:623-633.
40. Loeb M, Russell ML, Moss L, et al. Effect of influenza vaccination of children on infection rates in Hutterite communities: a randomized trial. *JAMA*. 2010;303:943-950.
41. Furuya-Kanamori L, Cox M, Milinovich GJ, Magalhaes RJS, Mackay IM, Yakob L. Heterogeneous and dynamic prevalence of asymptomatic influenza virus infections. *Emerg Infect Dis*. 2016;22:1052-1056.

SUPPORTING INFORMATION

Additional supporting information may be found in the online version of the article at the publisher's website.

How to cite this article: Otani Y, Kasai H, Tanigawara Y. Pharmacometric analysis of seasonal influenza epidemics and the effect of vaccination using sentinel surveillance data. *CPT Pharmacometrics Syst Pharmacol*. 2022;11:44–54. doi:10.1002/psp4.12732